Computational Modeling of Small-Scale Flow of Thixotropic Yield-stress Materials

Carlos E. Sanchez-Perez, Danmer Maza, Paulo R. de Souza Mendes, Marcio S. Carvalho

Department of Mechanical Engineering, Pontifícia Universidade Católica do Rio de Janeiro
Rua Marquês de São Vicente, 225, 22451-900, Rio de Janeiro, Brazil
csanchez@lmmp.mec.puc-rio.br, danmerm@puc-rio.br, pmendes@puc-rio.br, msc@puc-rio.br

Abstract. Computational modeling of flow of thixotropic yield-stress materials is challenging, because it requires an accurate model which should be able to describe the break and buildup of the material microstructure. Traditionally, thixotropic flows have been modeled by using very empirical equations which have a very restricted range of feasibility. Alternatively, in the present work, it is used a novel fluidity-based constitutive model that involves no postulated functions or parameters. Instead of using empirical parameters, this model involves measurable material functions whose parameters are obtained from data of standard experiments. Likewise it is more appropriate to describe the behavior of thixotropic material flows. In addition, the model assumes a one-to-one correspondence between the fluidity (i.e., the reciprocal of viscosity) and the microscopic state.

A numerical model of thixotropic yield-stress materials flowing through a capillary with a constriction is presented here. The complex flow is governed by the continuity and momentum equations coupled with two additional equations. One is a scalar evolution equation of fluidity while the other is a tensorial equation. The latter relates stress and strain rate. The system of equations was solved by using the Galerkin and Petrov-Galerkin / Finite Element Method.

The results show how fluidity , which represents the internal microstructure level, and velocity of thixotropic yield-stress liquids change inside the capillary. Both velocity and fluidity are a function of the flow behavior index, the yield stress and two material properties associated with different thixotropic characteristic-time scales: the avalanche time and the construction time.

Keywords: Thixotropy, Fluidity, Capillary, Finite Element Method, Avalanche and Construction times.

1 Introduction

Interesting and important fluids in industry and other human activities differ from the “ideal” Newtonian behavior. The mechanical behavior of structured fluids, such as polymeric solutions, waxy oils, muds, pharmaceutical & cosmetic products, paints, clay suspensions, processed food, among others (Mewis and Wagner [1], de Souza Mendes [2]) , cannot be described by a simple linear relationship between stress and rate of strain. Furthermore, despite of the extensive literature focused on coating of Newtonian fluids, most liquids in coating applications are strongly non-Newtonian (Glass and Prud’homme [3]). The macroscopic rheological properties of many of them rely on their microscopic structure (Pritchard et al. [4]). As a result, their rheology also has time dependency. For example, particle suspensions used in coating applications. However, time dependent behavior tends to be neglected and steady-state values are used instead.

Time-dependent fluids are subdivided into thixotropic and anti-thixotropic (or so-called rheopectic in some literature). Regarding to the thixotropic phenomenon, it is characterized by a gradual break down of the fluid internal microstructures under shear. On the other hand, these microstructures eventually build up when the flow is ceased. As a result, thixotropy is a reversible process but the microstructure change takes time (Barnes [5]).

Most of thixotropic models have a semi-empirical nature (Mewis and Wagner [1]). They are based on two equations: the stress (σ) as a function of the shear rate $\dot{\gamma}(t)$ and the yield stress σ_y, as shown in equation 1 and a kinetic-like equation, as described in equation 2. The latter shows the evolution of a structuring parameter (λ), where λ = 1 represents the maximum micro-structuring level while λ = 0 represents the minimum.

$$\sigma(t) = \sigma_y[\lambda(t)] + \eta_\lambda[\lambda(t), \dot{\gamma}(t)]\dot{\gamma}(t) + \eta_{\lambda=0}[\dot{\gamma}(t)]\dot{\gamma}(t) \quad (1)$$

$$\frac{d\lambda}{dt} = -k_1\dot{\gamma}^a\lambda^b + k_2\dot{\gamma}^c(1-\lambda)^d \quad (2)$$

The first term in the right-hand side of Eq. 1 is the yield stress, while η_λ and $\eta_{\lambda=0}$ are the structural and residual viscosities respectively. k_1, k_2, a, b, c and d are constants of the kinetic evolution equation.

de Souza Mendes [2], de Souza Mendes and Thompson [6, 7] and de Souza Mendes et al. [8] have used mechanical analogues, as shown in Figure 1, with the intention of unifying thixotropic models. In addition, de Souza Mendes et al. [8] replaced the structuring parameter (λ) for a more meaningful parameter: fluidity. Actually, the latter is the reciprocal of viscosity. Furthermore, this rheological model is based on parameters obtained experimentally. Previous works like Fredrickson [9] also proposed the use of fluidity instead of the structuring parameter.

Besides the thixotropic characterization, measurement and modeling; there are many challenges in incorporating these models into actual flow simulations. In the case of mixers, Barnes [5] argues that the simulations are relatively easy. Actually, the mixer is treated as a viscometer running at the same shear rate as the average shear rate in the mixer. On the other hand, the same author says that the simulation of flows in pipes is very complicated, especially in short ones where a steady-state condition is not reached. He also argues that the analysis is complex and extensive numerical methods are required. For instance, Moisés et al. [10] used the finite volume method to simulate start-up thixotropic flow in a horizontal pipe. Although Sochi [11] and others give some hints and identify issues to simulate thixotropic flows into porous media in small scale, the research related is much more limited. As a result, this is one of the main motivations of this work.

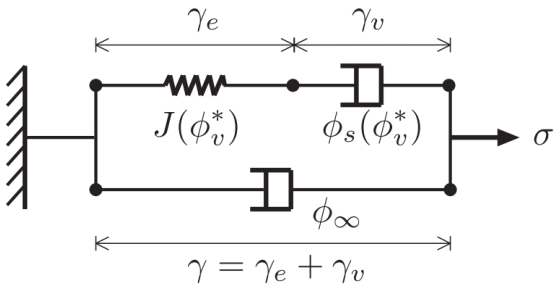

Figure 1. Mechanical Analogue of Thixotropic fluids (de Souza Mendes et al. [8])

2 Mathematical model and methodology

The mechanical analogue shown in Figure 1 is suitable for viscoelastic thixotropic fluids. Therefore, a tensorial Oldroyd-B-like differential equation (3) represents the model described just before. ϕ_v^* is the normalized fluidity, which varies from 0 to 1. Then, this parameter is related to ϕ_0 and ϕ_∞ (As shown in equation 5); which are respectively the fluidities at maximum and minimum structuring level. θ_s and θ_∞ are the relaxation and retardation times respectively in the tensorial equation 3.

$$\dot{\gamma} + \theta_\infty(\phi_v^*)\overset{\triangledown}{\dot{\gamma}} = [(\phi_\infty - \phi_0)\phi_v^* + \phi_0]\left[\sigma + \theta_S(\phi_v^*)\overset{\triangledown}{\sigma}\right] \quad (3)$$

$$\text{where,} \quad \overset{\triangledown}{M} = \frac{DM}{Dt} - \boldsymbol{M}\cdot(\nabla\mathbf{v}) - (\nabla\mathbf{v})^T\cdot\boldsymbol{M} \quad (4)$$

$$\phi_v^* = \frac{\phi_v - \phi_0}{\phi_\infty - \phi_0} \quad (5)$$

The operator D/Dt in Eq. 4 represents a material time derivative. It is assumed that the normalized fluidity, ϕ_v^*, is governed by the evolution equation shown as follows:

$$\frac{D\phi_v^*}{Dt} = f\left[\phi_{eq}^*(\sigma), \phi_v^*\right] \quad (6)$$

ϕ^*_{eq} (See equation 7) is the normalized fluidity at equilibrium state, where K and n are the consistency and flow behavior indexes respectively. The function $f\big[\phi^*_{eq}(\sigma), \phi^*_v\big]$, as shown in equation (8), is obtained by rheological tests and described with more details in de Souza Mendes et al. [8]. The parameters s, t_a and t_c are a scalar exponent, avalanche and construction times respectively.

$$\phi^*_{eq} = \frac{\frac{1}{\sigma}\left[\frac{|\sigma-\sigma_y|}{K}\right]^{1/n}}{(\phi_\infty - \phi_0) + \frac{1}{\sigma}\left[\frac{|\sigma-\sigma_y|}{K}\right]^{1/n}} \tag{7}$$

$$f\big[\phi^*_{eq}, \phi^*_v\big] = \begin{cases} \frac{s}{t_a \phi^*_{eq}(\sigma)} \left(\phi^*_{eq} - \phi^*_v\right)^{\frac{s+1}{s}} {\phi^*_v}^{\frac{s-1}{s}} & \text{if } 0 < \phi^*_v \leq \phi^*_{eq} \\ -\frac{(\phi^*_v - \phi^*_{eq})}{t_c} & \text{if } \phi^*_{eq} < \phi^*_v \leq 1 \end{cases} \tag{8}$$

For the laponite suspension, obtained by de Souza Mendes et al. [8], t_c is usually a constant value while t_a is calculated by using the following equation:

$$t_a = 59.2 \frac{(1-\phi^*_{eq})^{1.1}}{{\phi^*_{eq}}^{0.4}}. \tag{9}$$

We are preliminarily studying thixotropic without a viscoelastic component. Consequently, equation (3) becomes much simpler, since θ_S and θ_∞ tend to be zero. In addition, de Souza Mendes et al. [8] founded that the laponite suspension did not have viscoelasticity associated. As a result, equation (3) takes the following form:

$$\dot{\gamma} = \phi_v \sigma. \tag{10}$$

Regarding to equation (6), we kept the convective transient term. Then, equation (11 is used to study the time dependency from the Lagrangian point of view.

$$\mathbf{v} \cdot \nabla \phi^*_v = f\big[\phi^*_{eq}(\sigma), \phi^*_v\big]. \tag{11}$$

There is still an issue with the continuity of $f\big[\phi^*_{eq}(\sigma), \phi^*_v\big]$, which was solved by using a smooth Heaviside function. The velocity $\mathbf{v}$ and pressure p of the incompressible flows are governed by the mass conservation equation $\nabla \cdot \mathbf{v} = 0$, and momentum equation $\rho(\mathbf{v} \cdot \nabla \mathbf{v}) - \nabla \cdot \mathbf{T} = 0$. Where ρ is the density of the liquid. The total stress tensor for Generalized Newtonian liquids is $\mathbf{T} = -p\mathbf{I} + \eta[(\nabla \mathbf{v}) - (\nabla \mathbf{v})^T]$ where η is the viscosity of the liquid (the reciprocal of the local ϕ). With the appropriate boundary conditions, the system of equations is solved by using the Galerkin and Petrov-Galerkin / Finite Element Method with quadrilateral finite elements.

3 Results and Discussion

The results were obtained by using the following rheological parameters: K = 1 Pa.s^n, n = 0.32, σ_y = 6 Pa, ϕ_∞ = 64.1 (Pa.s)$^{-1}$, which corresponds to a real laponite suspension (de Souza Mendes et al. [8]). The related normalized fluidity is shown in Figure 2.

The appropriate boundary conditions are necessary to solve the system of equations showed before. For the fluidity field, we imposed a constant fluidity ϕ_{IN} at the capillary inlet. In addition, we imposed a parabolic velocity profile at this position. At the capillary wall, the non-slip condition is used and an appropriate boundary condition is considered for the symmetry axis. Our geometry also includes a constriction. The fluid domain was discretized in a refine mesh concentrated on the capillary wall, symmetry axis as well as at the capillary inlet. Figure 3 shows the mesh of the constricted capillary used in the simulations.

A fluidity field of thixotropic flow through the constricted capillary is shown on Figure 4. In this case, we used all rheological parameters that we listed before. In addition, ϕ_{IN} was fixed in 1.0 (Pa.s)$^{-1}$. A volumetric flow rate (Q) of 7.5$\times$10^{-2} mm^3/s was also imposed. The avalanche time (t_a) was estimated by using the Eq. (9) while the construction time was fixed in 663 s; according to de Souza Mendes et al. [8]'s work.

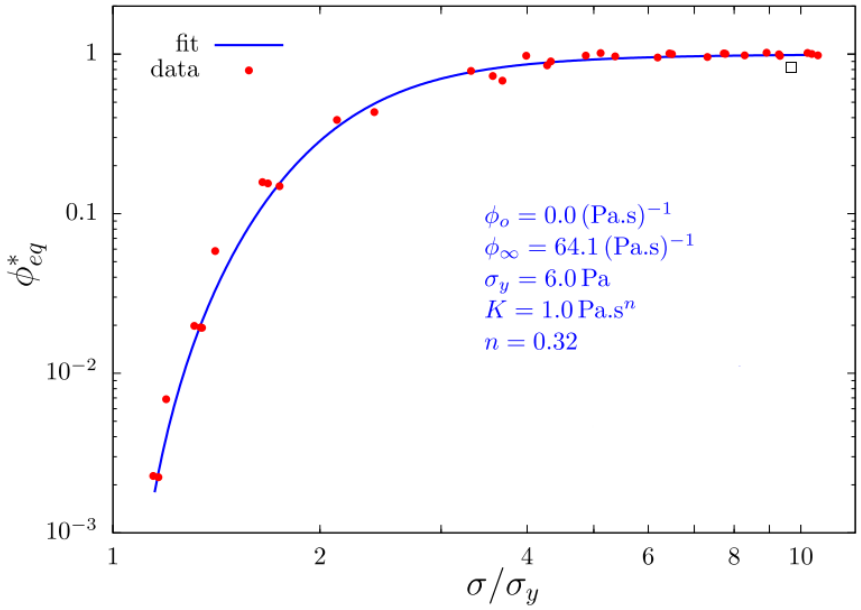

Figure 2. Normalized fluidity for a real laponite suspension obtained by de Souza Mendes et al. [8].

The destruction of the microstructure is usually observed at the capillary wall, since the fluid is under high stress. On the other hand, the build-up of microstructure usually happens in the region close the symmetry axis as the stress is much lower in this region. Since the construction time is very high compared to the liquid's residence time, it does not have enough time to buildup a significant quantity of microstructure. Therefore, the lowest values of fluidity are not achieved. It is important to notice that low values of ϕ_v represent high local values of viscosity because the fluidity is the reciprocal of viscosity.

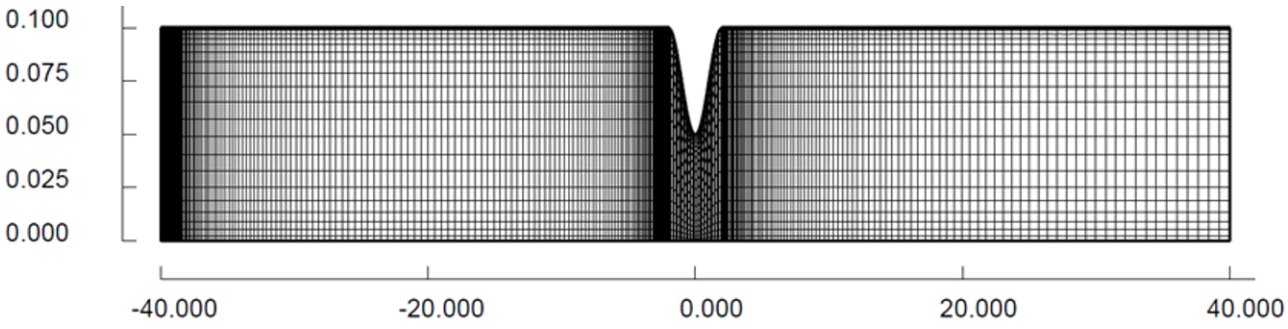

Figure 3. Mesh used for the constricted capillary

To obtain the fluidity fields shown in Figure 5 a) and b), we fixed both t_a and t_c. Likewise, a parametric analysis was done. Firstly, at Figure5 a), is shown a fluidity field with large avalanche and construction times of 150s and 663s respectively. This case is related to a more realistic thixotropic flow. Then, the characteristic times of the fluid were decreased as much as possible. As result, we obtained a fluidity field with avalanche and construction times equal to 3s, as shown in Fig.5 b). The idea is to achieve a condition which tends to an equilibrium which is shown in Fig.5 c). Likewise, the hypothetical flow of short characteristic time-liquid is more closely related to generalized Newtonian model (GNM); where time dependency is not considered.

Then, it is possible to observe many differences between both cases a) and b): large and short characteristic times of the fluid respectively. On the fluidity field of Figure 5 b), it is possible to appreciate two highlighted areas: unstructuring-region nearby the capillary wall while a building up region close to the symmetry axis. The stress affects directly the structuring level of the thixotropic fluid, which is expressed by means of the fluidity values. Since the fluid is under much more stress, close the capillary wall and constriction, its microstructure tends to be

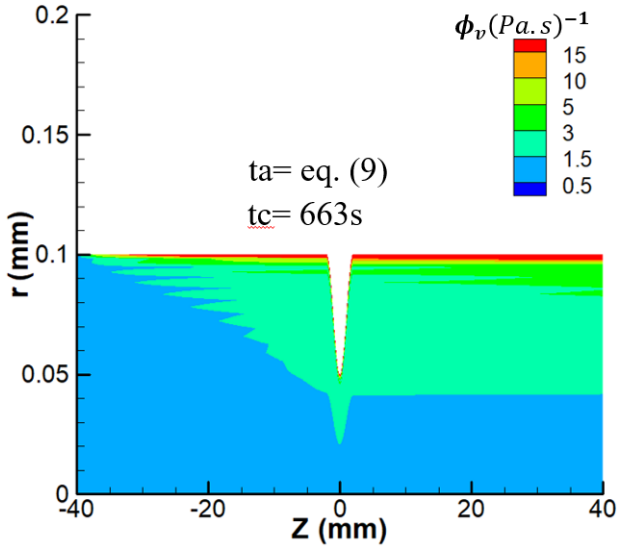

Figure 4. Fluidity field of a laponite suspension through a constricted capillary

destroyed close to these regions. Then, this phenomenon is expressed by high values of fluidity. On the other hand, close to capillary axis, the stress is much lower. As a result, the microstructure tends to be constructed and low values of fluidity are reflected there.

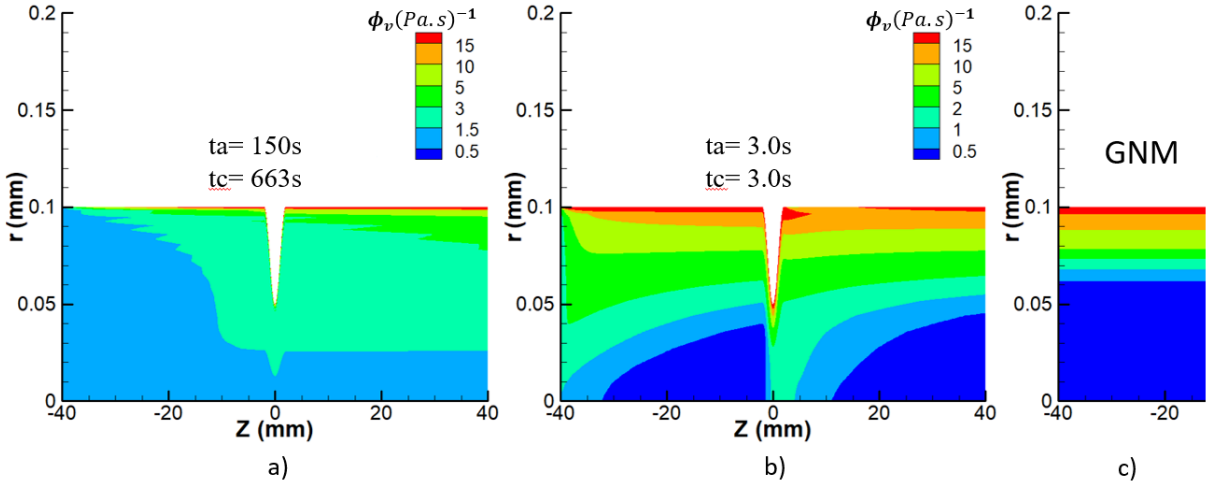

Figure 5. Fluidity fields of two hypothetical flows: large and short characteristic times, and that obtained by the GNM model.

The changes in fluidity, along the domain, affect other important parameters like pressure drop as reflected in Figure 6. In this graph, the pressure profiles of three different flow cases are compared. Firstly, the thixotropic flow shown in Figure 4 (blue line). Secondly, the hypothetical thixotropic flow shown in Figure 5 b) (red line). Then, a pressure profile obtained by using the GNM model corresponding to Equation (7) (green line). All of them are at the same flow rate condition.

The higher levels of stress on the GNM flow, close to the capillary wall and constriction, produces higher values in fluidity compared to those for the thixotropic flow (represented by high characteristic times). Since fluidity is the reciprocal of viscosity, GNM predicts lower values of viscosity at the capillary wall. Then, a lower effect of friction is expected as lower values of pressure drop according to the GNM model.

From this result, the pressure profile obtained with low values of characteristics times, ta and tc equal to 3s, shows very similar values to those whose corresponds to the GNM model profile; especially after the constriction.

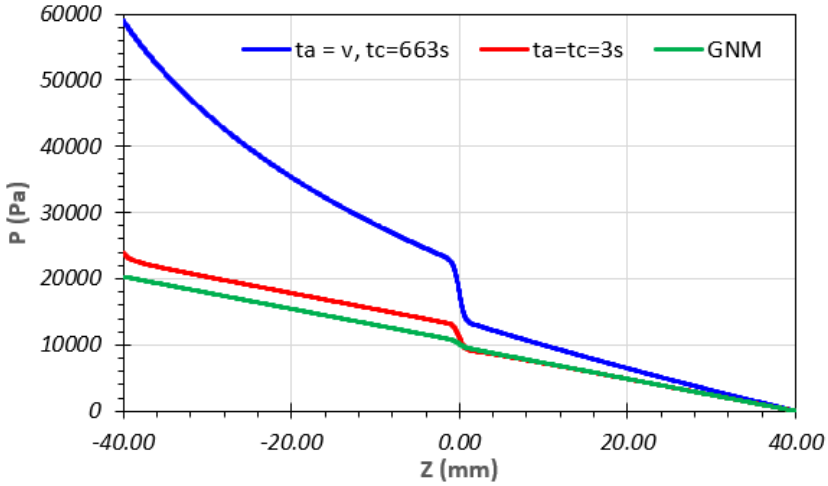

Figure 6. Pressure profiles for the thixotropic model and for GNM model of a laponite suspension

4 Conclusions

A novel rheological model, based on fluidity, was used. The system of equations that consists of continuity, momentum and fluidity equations was solved by using the Galerkin and Petrov-Galerkin / Finite Element Method. As a result, fluidity fields, velocity and pressure profiles were obtained for laponite suspension into a capillary.

Most flow analyses of particle suspensions oversimplify the rheological modeling. For instance, the use of simple viscosity equations like generalized Newtonian models. Furthermore, neglecting time dependency, by only considering viscosity as a function of the local shear rate, may completely misrepresent the flow phenomena. Consequently, time dependency should be considered in thixotropic flows to model them accurately.

Authorship statement. The authors hereby confirm that they are the sole liable persons responsible for the authorship of this work, and that all material that has been herein included as part of the present paper is either the property (and authorship) of the authors, or has the permission of the owners to be included here.

References

[1] J. Mewis and N. J. Wagner. Thixotropy. *Advances in Colloid and Interface Science*, vol. 147-148, pp. 214–227. Colloids, polymers and surfactants.Special Issue in honour of Brian Vincent, 2009.

[2] P. R. de Souza Mendes. Modeling the thixotropic behavior of structured fluids. *Journal of Non-Newtonian Fluid Mechanics*, vol. 164, n. 1, pp. 66–75, 2009.

[3] J. E. Glass and R. K. Prud'homme. *Coating Rheology: Component Influence on the Rheological Response and Performance of Water-Borne Coatings in Roll Applications*, pp. 137–182. Springer Netherlands, Dordrecht, 1997.

[4] D. Pritchard, S. K. Wilson, and C. R. McArdle. Flow of a thixotropic or antithixotropic fluid in a slowly varying channel: The weakly advective regime. *Journal of Non-Newtonian Fluid Mechanics*, vol. 238, pp. 140–157. Viscoplastic Fluids From Theory to Application 2015 (VPF6), 2016.

[5] H. A. Barnes. Thixotropy—a review. *Journal of Non-Newtonian Fluid Mechanics*, vol. 70, n. 1, pp. 1–33, 1997.

[6] P. R. de Souza Mendes and R. L. Thompson. A critical overview of elasto-viscoplastic thixotropic modeling. *Journal of Non-Newtonian Fluid Mechanics*, vol. 187-188, pp. 8–15, 2012.

[7] P. R. de Souza Mendes and R. L. Thompson. A unified approach to model elasto-viscoplastic thixotropic yield-stress materials and apparent yield-stress fluids. *Rheologica Acta*, vol. 52, pp. 673–694, 2013.

[8] P. R. de Souza Mendes, B. Abedi, and R. L. Thompson. Constructing a thixotropy model from rheological experiments. *Journal of Non-Newtonian Fluid Mechanics*, vol. 261, pp. 1–8, 2018.

[9] A. G. Fredrickson. A model for the thixotropy of suspensions. *AIChE Journal*, vol. 16, n. 3, pp. 436–441, 1970.

[10] G. Moisés, L. Alencar, M. Naccache, and I. Frigaard. The influence of thixotropy in start-up flow of yield stress fluids in a pipe. *Journal of Petroleum Science and Engineering*, vol. 171, pp. 794–807, 2018.

[11] T. Sochi. Non-newtonian flow in porous media. *Polymer*, vol. 51, n. 22, pp. 5007–5023, 2010.